ELSEVIER

The sedimentary fluxes of polycyclic aromatic hydrocarbons in the Yangtze River Estuary coastal sea for the past century

Zhigang Guo [a,*], Tian Lin [b], Gan Zhang [b], Mei Zheng [c], Zongyan Zhang [a], Yunchao Hao [a], Ming Fang [d]

[a] College of Marine Geosciences, Ocean University of China, Qingdao, 266100, China
[b] State Key Laboratory of Organic Geochemistry, Guangzhou Institute of Geochemistry, Chinese Academy of Sciences, Guangzhou, 510640, China
[c] School of Earth and Atmospheric Sciences, Georgia Institute of Technology, Atlanta, Georgia 30332, USA
[d] Department of Chemical Engineering, The Hong Kong University of Science & Technology, Clearwater Bay, Hong Kong, China

Abstract

Polycyclic aromatic hydrocarbons (PAHs) in two ^{210}Pb dated sediment cores from the coastal East China Sea, strongly influenced by the discharge from the Yangtze River, were determined to help to reconstruct the economic development over the past century in East China. The variations in PAH concentrations and fluxes in the sediment cores were primarily due to energy structure change, severe floods and dam construction activities. The impact on PAHs by the river discharge overwhelmed the atmospheric depositions. The profiles of PAH fluxes and concentrations as well as compositions in the cores revealed the transformation from an agricultural economy to an industrial one especially after the 1990s' in the region. PAHs in the study area were dominated by pyrolytic sources.
© 2007 Elsevier B.V. All rights reserved.

Keywords: Pyrolytic PAHs; Sediment cores; Sedimentary flux; Source; Yangtze River Estuary coastal sea

1. Introduction

Polycyclic aromatic hydrocarbons (PAHs), an important class of organic pollutants and known carcinogens and mutagens, are ubiquitous in the environment. PAHs are mainly attributed to combustion processes including the burning of fossil fuels, municipal wastes and biomass (Yunker et al., 2002; Oros and Ross, 2004). Other sources include crude oil seepage and diagenesis of organic matter in anoxic sediments (Venkatesan, 1988; Lima et al., 2005). PAH in China is a severe problem. For example, the emission of 16 priority PAHs proposed by the United States Environmental Protection Agency (16 PAHs) reached 23,300 t in 2003 (Xu et al., 2006) largely due to the increasing use of coal, petroleum and biomass for energy to meet the rapid economic growth.

The Yangtze River is the world's fifth largest river in water discharge (9200 Mt yr^{-1}) and historically the fourth largest one in sediment discharge at 480 Mt yr^{-1} (Yang et al., 2006). It discharges into the East China Sea (ECS) and the sediments are deposited mainly in the Yangtze River Estuary (YRE) and the coastal mud off

* Corresponding author. Tel./fax: +86 532 6678 2062.
  E-mail address: guozgg@ouc.edu.cn (Z. Guo).

Zhejiang and Fujian Provinces (CMZF) due to the Coriolis effect and circulation system (Hu and Yang, 2001) (Fig. 1). YRE and CMZF are sinks for the fine-grained sediments and the associated pollutants from the Yangtze River.

There are several reports of PAHs in the ECS in the literature, including PAHs in surface sediments (Bouloubassi et al., 2001) and in an inter-tidal flat core, reflecting the influence of a nearby sewage outlet based on the historical concentration trends of PAHs (Liu et al., 2000). Recently, Guo et al. (2006) reported that the atmospheric depositional fluxes of the 16 PAHs in the central ECS shelf in 2001 were 5.3 times higher than

that before industrialization ($\sim$1850). In this paper, sedimentary fluxes of PAHs for the past century in two ^{210}Pb dated sediment cores from YRE and north CMZF are discussed to reveal the impact of the anthropogenic activities around the Yangtze River drainage basin on the coastal ECS.

2. Methods

2.1. Sample collection

Two sediment cores were collected using a gravity corer deployed from the R/V Dong Fang Hong 2 of the
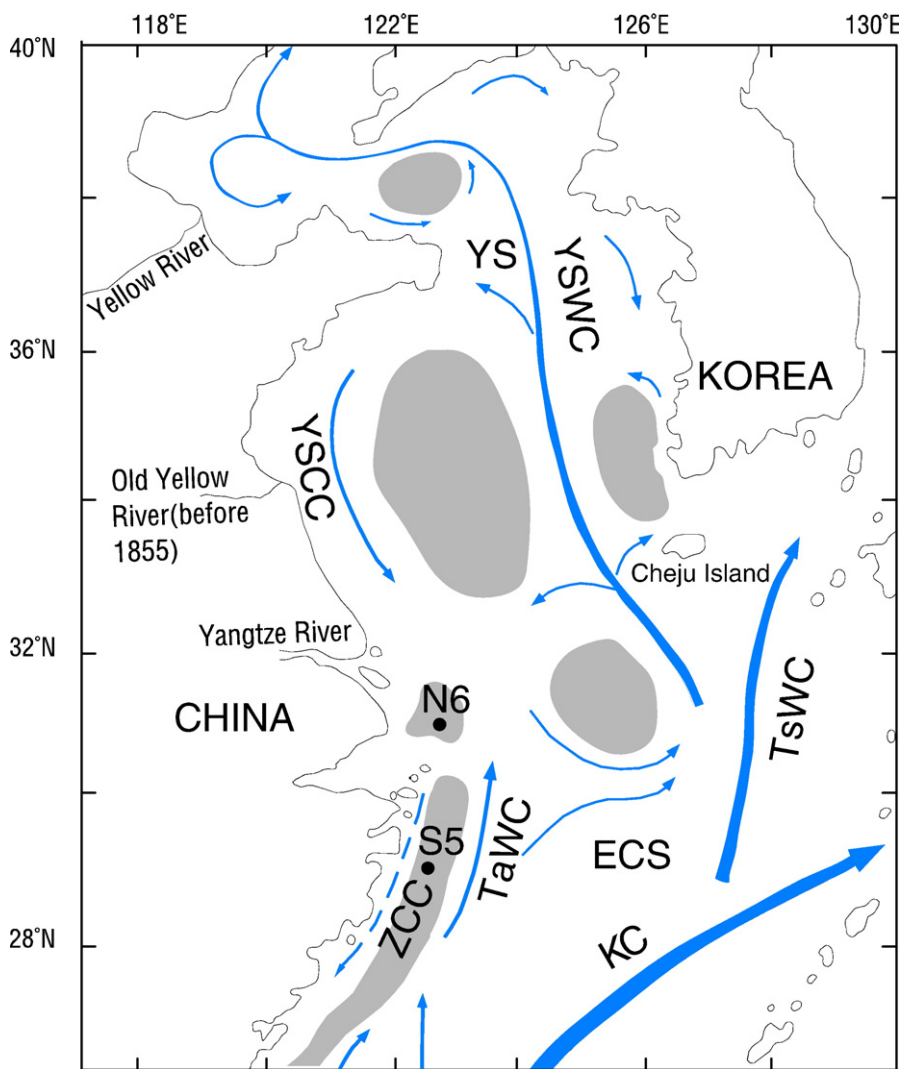

Fig. 1. Sampling sites and the general circulation systems in the Yellow Sea and East China Sea. ECS: East China Sea; YS: Yellow Sea; KC: Keroshio Current; TaWC: Taiwan Warm Current; TsWC: Tsushima Warm Current; YSCC: Yellow Sea Coastal Current; YSWC: Yellow Sea Warm Current. ZCC: Zhejiang Coastal Current. Circulation systems and mud areas (dark areas) are after Hu and Yang (2001).

Ocean University of China in June 2003. N6 (122°44.37′ E, 30°30.44′N) was located in the YRE and the water depth was 41.3 m; S5 (122°30.01′E, 29°00.25′N) was located in northern CMZF and the water depth was 50.0 m (Fig. 1). The cores were cut into 2 cm sections along the length using a stainless steel cutter in the laboratory. The samples were packed in aluminum foil and stored at −20 °C until analysis.

2.2. Measurement of the dry density of the sediments

A pre-cleaned and pre-weighted stainless steel specimen ring (59.96 cm^3, 2 cm in height, 6.18 cm in diameter) was used to collect samples from the wet sediment cores for dry density measurement. After weighing the total wet sample, about one eighth of the wet sample was dried in a 110 °C oven for 24 h for dry weight measurement.

2.3. Sediment dating

The dominant fallout of ^{210}Pb in the ECS was from the wet and dry atmospheric depositions because the riverine particles had low ^{210}Pb activities, and the water column (30-70 m) is too shallow to allow the decay of ^{226}Ra in the seawater to ^{210}Pb (DeMaster et al., 1985).

The N6 sediment core was dated based on the method by Wu et al. (2006) at the Nanjing Institute of Geography and Limnology. The activities of ^{137}Cs were too low to yield any confident results, therefore only ^{210}Pb dating was used in this study. ^{210}Pb and ^{226}Ra activities were measured using an Ortec HPGe GWL series well-type coaxial low background intrinsic germanium detector. ^{210}Pb was determined by gamma emissions at 46.5 keV, and ^{226}Ra by 295 keV and 352 keV gamma rays emitted by the daughter isotope ^{214}Pb following 3 weeks of storage in sealed containers to allow radioactive equilibration. ^{210}Pb$_{ex}$ was calculated by subtracting ^{226}Ra activities from the total ^{210}Pb activities. The relative error for this method was <10%. The S5 sediment core was dated at the Guangzhou Institute of Geochemistry following the method by Zhang et al. (2002). ^{210}Pb activities were determined by analyzing the radioactivity of the decay product ^{210}Po by assuming that the two were in equilibrium. Po was extracted, purified, and self-plated onto silver disks. Po was used as the yield monitor and tracer in quantification. Counting was conducted by computerized multi-channel α spectrometry with gold-silicon surface barrier detectors. The relative error for this method was less than 6%. Constant sedimentation rates of 3.38 cm yr^{-1} at site N6 and 0.98 cm yr^{-1} at site
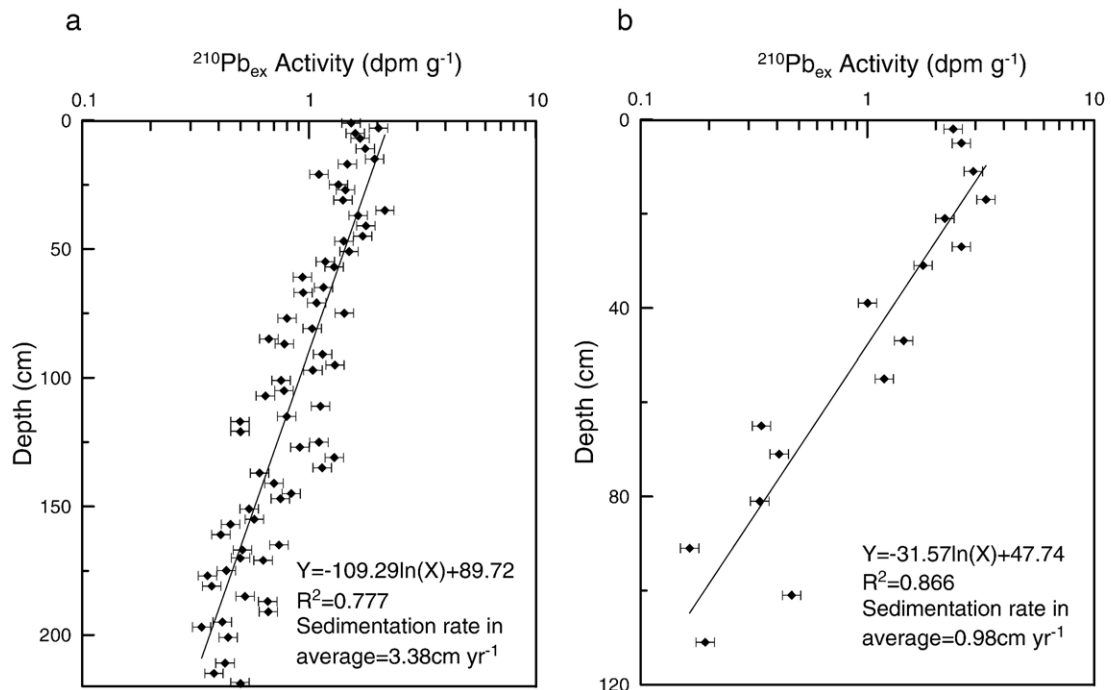

Fig. 2. ^{210}Pb dating of (a) N6 and (b) S5.

S5were calculated using the constant activity (CA) model (Fig. 2). The results are in agreement with those reported by DeMaster et al. (1985) and Huh and Su (1999) in the same area. The data for S5 beyond 100 yr are used only as a reference.

2.4. Organic analysis

The PAH analytical procedure and QA/QC followed that described by Mai et al. (2003). Briefly, ~10 g of the sample was spiked with a mixture of recovery standards of five deuterated PAHs. The samples were extracted with dichloromethane in a Soxhlet extractor for 72 h, with activated copper added to remove the sulfur in the samples. The extract was concentrated and fractionated using a silica–alumina (1:1) column. PAHs and polar components were eluted using 35 ml of hexane/dichloromethane (1:1) and 25 ml of methanol, respectively. Hexamethylbenzene was added as internal standard and the mixture was reduced to 0.2 ml and subjected to GC-MSD (a HP-5972 mass spectrometer interfaced to a HP-5890 II gas chromatography) analysis. The GC was equipped with a HP-5 capillary column (25 m × 0.25 mm id, film thickness 0.25 μm) with helium as carrier gas. The GC operating conditions were: held at 80 °C for 5 min, ramped to 290 °C at 4 °C min^{-1} and held for 30 min. The sample was injected splitless with the injector temperature at 290 °C. The MSD was operated in the electron impact (EI) mode at 70 eV and the selected-ion-monitoring (SIM) mode. Procedural blanks, standard-spiked blanks, standard-spiked matrix and parallel samples were analyzed for quality assurance and control. The recovery for core N6 was 38.3 ± 10.3% for naphthalene-d$_8$, 70.0 ± 7.8% for acenaphthene-d$_{10}$, 103.4 ± 12.0% for phenanthrene-d$_{10}$, 56.2 ± 10.8% for chrysene-d$_{12}$ and 45.5 ± 12.8% for perylene-d$_{12}$, and for core S5 it was 62.7 ± 11.2%, 68.4 ± 14.4%, 95.0 ± 23.3%, 93.3 ± 19.7% and 99.8 ± 19.8%, respectively. The PAH concentrations were recovery corrected sample by sample so that the data of the two cores can be compared. Procedural blank samples contained no detectable amount of the PAHs targeted. The relative percent analysis difference of paired duplicate samples was <15% (n = 5). Method detection limits for individual PAHs ranged from 0.2 to 2 ng g^{-1} (Mai et al., 2003). The 21 PAHs measured were: naphthalene (NAP), acenaphthylene (AC), acenaphthene (ACE), fluorene (FLU), phenanthrene (PHE), methylphenanthrene (MP), dimethylphenanthrene (DMP), trimethylphenanthrene (TMP), quatermethylphenanthrene (QMP), anthracene (ANT), fluoranthene (FLUO),

pyrene (PYR), benz[*a*]anthracene (BaA), chrysene (CHR), benzo[*b*]fluoranthene (BbF), benzo[*k*]fluoranthene (BkF), benzo[*a*]pyrene (BaP), indeno[*1,2,3-cd*]pyrene (INP), dibenz[*a,h*]anthracene (DBA), perylene (PER) and benzo[*ghi*]perylene (BghiP).

3. Results and discussion

3.1. Down-core flux variation of 16 PAHs

The sedimentary flux and concentration profiles of 16 PAHs in the two cores are shown in Fig. 3. The individual PAH sedimentary flux was calculated from the corresponding concentration, the average sedimentary rate and the dry density of the sediment. The sediment focusing factor is less than 1.2 in the Yangtze River Estuary coastal sea (Huh and Su, 1999), thus, the sedimentary inventories do not greatly exceed the amounts from ^{210}Pb atmospheric fallout (Lima et al., 2003). PAH fluxes were not corrected for sediment focusing in this work because the particle–associated PAHs in the samples were mainly from the Yangtze River discharge with only a minor contribution from atmospheric deposition (Bouloubassi et al., 2001).

Although the concentrations of the 16 PAHs after the 1990s were significantly higher than those in N6, the sedimentary fluxes were just the opposite. The relatively low concentrations of the 16 PAHs in N6 were attributed to the diluting effect of the much higher sedimentation rate (3.38 cm yr^{-1}).

The sedimentary flux of the 16 PAHs in N6 showed a slow increase from the 1930s to the 1970s but there was an obvious decrease (average 144 ng cm^{-2} yr^{-1} and range 115–203 ng cm^{-2} yr^{-1}) in the 1980s, even lower than that for the 1930s (Fig. 3). Since the 1990s, the sedimentary flux experienced a huge increase, reaching the highest value of 408 ng cm^{-2} yr^{-1} in ~2002. The sedimentary fluxes in S5 were low before the 1940s. After the founding of the People's Republic of China in 1949, the flux increased and reached a peak in the middle of the 1950s (152 ng cm^{-2} yr^{-1}) before decreasing somewhat in the 1960s. The flux increased again in the 1970s and reached 184 ng cm^{-2} yr^{-1} before dropping in the 1980s. The flux increased once more in the beginning of the 1990s and reached the highest value of 199 ng cm^{-2} yr^{-1} in ~1999. The variation of the 16 PAH fluxes in N6 and S5 from the beginning of 1990s to the present followed the economic development in China very well. The rapid, strong and sustained economic development since the 1980s needed a large amount of energy, viz., coal and petroleum, resulting in a huge increase in the emission of PAHs.
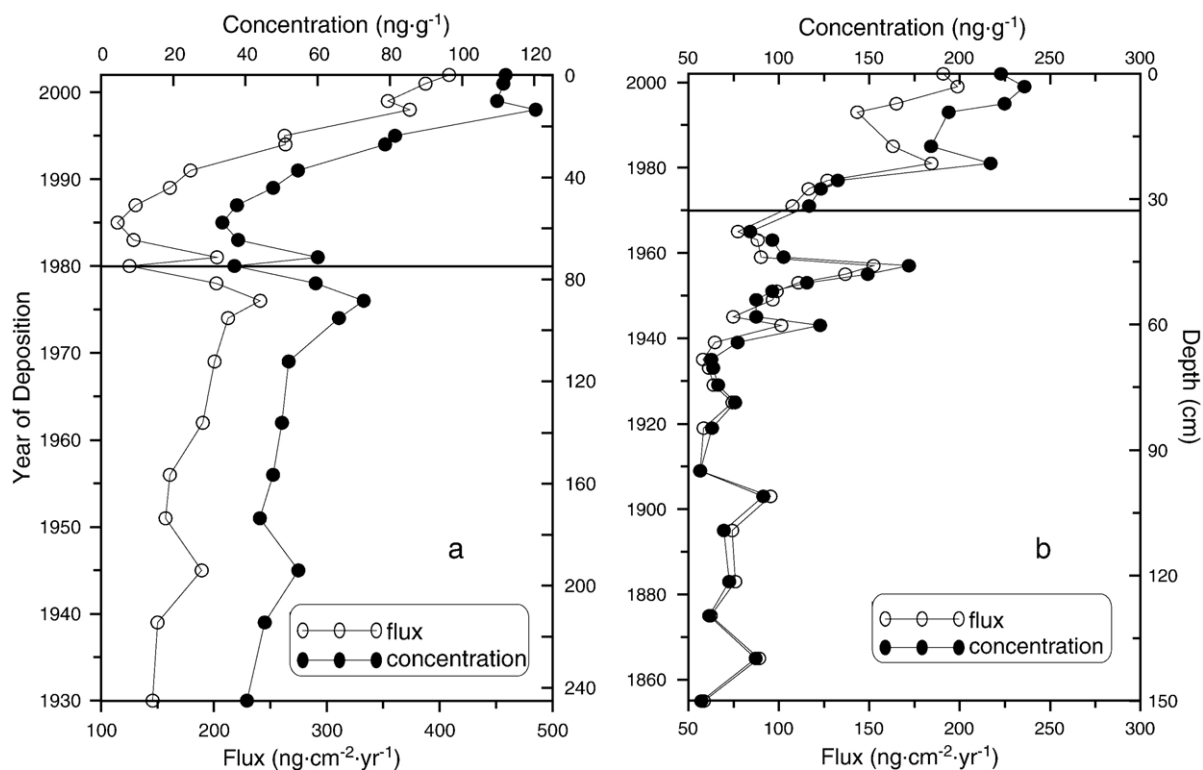
Fig. 3. Down-core concentrations (upper *x*-axis) and fluxes (bottom *x*-axis) of the 16 USEPA priority PAHs in (a) N6 and (b) S5.

There were two 16 PAH flux peaks in S5 in the mid-1950s and in ~1999 while for N6 only one PAH concentration peak with a small flux peak in ~1998 was observed. The two flux peaks were probably due to the severe Yangtze River floods in 1954 and 1998 (Yang et al., 2006). The excessive stripping and leaching by the flood water transported much more PAHs accumulated in soil and water system (*e.g.*, reservoirs and lakes) in the drainage basin of the Yangtze River into the ECS. During the severe flood years, the sediment discharge was relatively low when compared to the water discharge, which could be attributed to the large amount of sediment loss in the middle reaches due to the river breaches and over-bank flows, especially in the Jingjiang fluvial plain (Yang et al., 2006). The sediment discharge was mainly from the upper reaches in the edge of Tibet in southwest China, while the pollutants including PAHs were chiefly from the middle and lower reaches due to dense population and high level of industrialization, especially in the Yangtze River Delta.

There was a period of low 16 PAH flux in both N6 and S5 in the 1980s. This could be related to the huge dam construction activities in the upper and middle streams of the Yangtze River in the 1970s and 1980s. Up to 1995, there were 45,628 reservoirs, including of 119 large ones in the river system, and most of them were built in the 1970s and 1980s (Yang et al., 2006). This could result in the decrease in the 16 PAH flux from the Yangtze River into the ECS because much particle-associated PAHs could be retained by the dams.

These results indicate that the temporal 16 PAH flux distributions of the coastal ECS are strongly influenced by the Yangtze River discharge and the modification of the water system, suggesting that the PAHs originate mainly from the Yangtze River drainage basin (Bouloubassi et al., 2001).

3.2. Sources of the PAHs

ANT/(ANT+PHE) <0.1 and BaA/(BaA+CHR) <0.2, have been suggested for petrogenic sources, and for pyrolytic sources, these ratios would be >0.1 and >0.35, respectively (Yunker et al., 2002). ANT/(ANT+PHE) was 0.06–0.13 for N6 and 0.03–0.09 for S5, indicating that some of the PAHs were petrogenic, especially in S5. BaA/(BaA+CHR) was 0.28–0.44 in N6 and 0.31–0.50 in S5, indicating that pyrolytic source was dominant at both sites except in some layers where
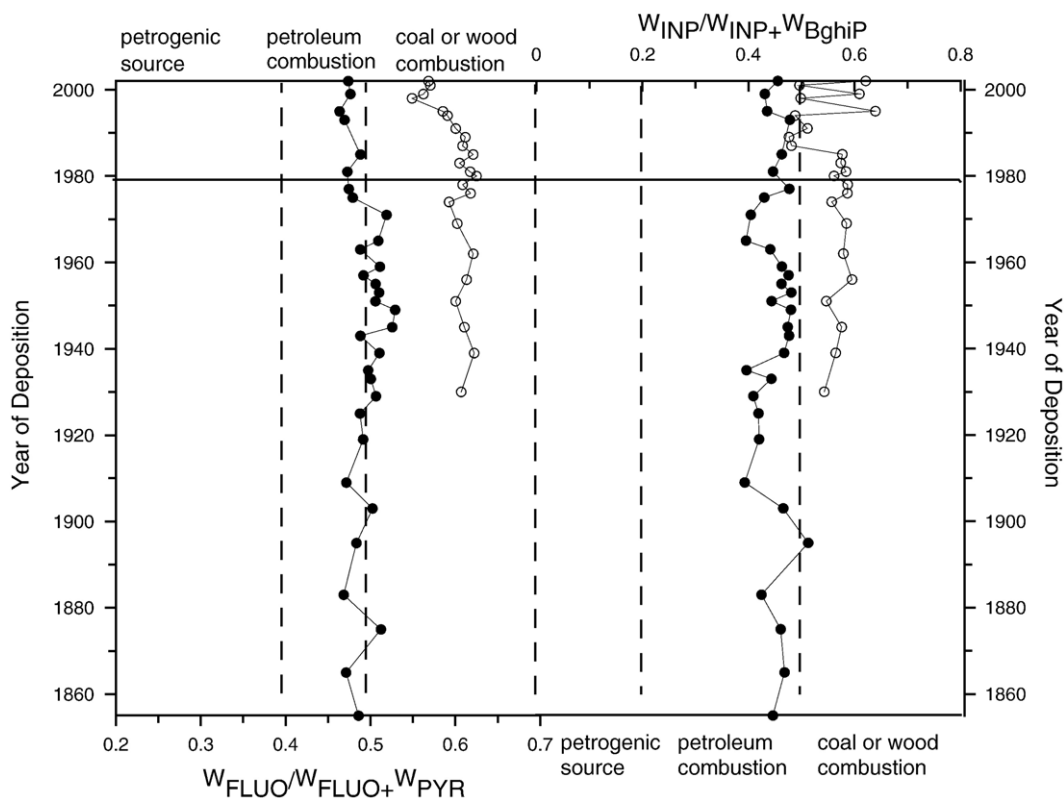
Fig. 4. Source identification using PAH ratios; N6 (open circles) and S5 (solid circles). FLUO/(FLUO+PYR) <0.4=petrogenic source, 0.4–0.5=liquid fossil fuel combustion, >0.5=coal, grass or wood combustion; INP/(INP+BghiP) <0.2=petrogenic, 0.2–0.5=liquid fossil fuel combustion, >0.5=coal, grass and wood combustion (Yunker et al., 2002; Mai et al., 2003).

some of the PAHs could be petrogenic. Pyrolytic PAHs have MP/PHE <1 while it is 2–6 for petrogenic PAHs (Mai et al., 2003). For N6, MP/PHE was 0.51–0.77 and 0.25–0.46 for S5, suggesting that pyrolytic source was dominant in both YRE and north CMZF.

FLUO/(FLUO+PYR) and INP/(INP+BghiP) profiles are shown in Fig. 4. These results suggested that pyrolytic PAHs in the YRE were mainly from the coal and/or grass and wood combustion while these PAHs in the northern CMZF were from mixed sources of petroleum and coal and/or grass and wood combustion. FLUO/(FLUO+PYR) showed a decreasing trend since the 1980s at N6 and since the 1970s at S5, especially after the 1990s, implying an increase of petroleum combustion contribution of PAHs to the ECS. Due to the rapid economic development in the Yangtze River Delta, the enhanced emission of PAHs from automobiles to the coastal ECS should be expected.

Principal Component Analysis (PCA) was used for source apportionment. Based on the loading of all 21 measured PAHs (55 samples, total), three principal components (PC1, PC2 and PC3) were identified, accounting for 72.0%, 16.3% and 5.4%, respectively, of the total variance. The results are shown in Fig. 5. Low molecular weight PAHs (NAP, AC, ACE, FLU, PHE, MP, DMP, TMP, QMP, PYR and ANT) had negative PC2 but high PC1 attributable to petrogenic and low-moderate temperature pyrolytic sources (Mai et al., 2003). High molecular weight PAHs (FLUO, BaA, CHR, BbF, BkF, BaP, INP, DBA and BghiP) had high PC1 as well as positive PC2 suggesting high temperature combustion sources (Mai et al., 2003). PER was a special case, with high in PC3 and low in PC1. PER is usually attributed to the diagenesis of organic matter in anoxic marine sediments (Venkatesan, 1988).

3.3. Compositional flux variation of 16 PAHs

Normalized fluxes of 2+3-ring (NAP, AC, ACE, FLU, PHE and ANT), 4-ring (FLUO, PYR, BaA and CHR), 5+6-ring (BbF, BkF, BaP, INP, DBA and BghiP) PAHs and BaP are shown in Fig. 6. Before 1990, the
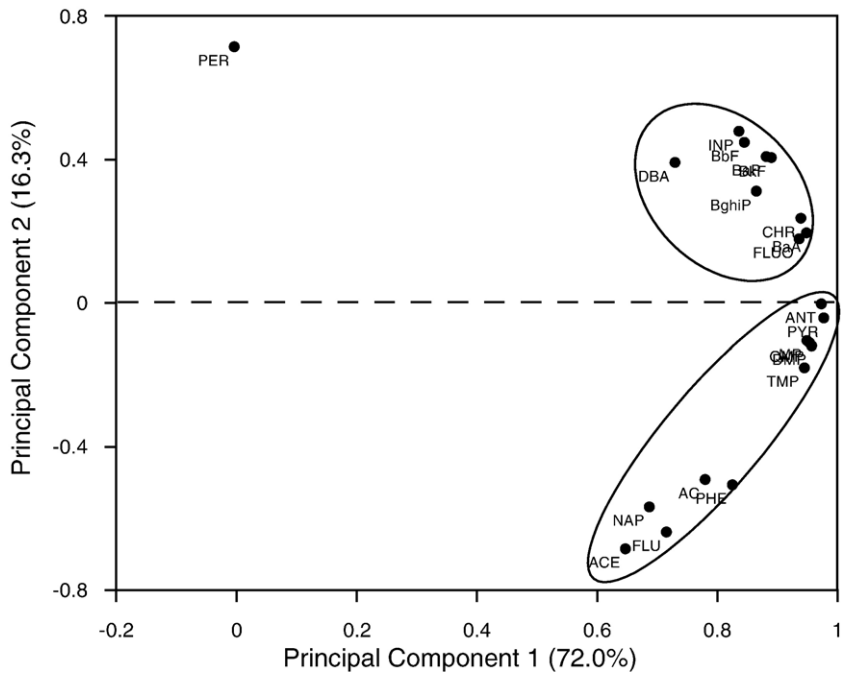
Fig. 5. Principal component analysis of PAHs.

variation of these normalized values was small in N6, but much larger increases were observed in subsequent years. The increase was highest for the 5+6-ring PAHs

and lowest for the 2+3-ring PAHs. BaP, a toxic compound, was ~8 times higher than that in ~1930. The same trend can be seen since the late 1970s for S5.
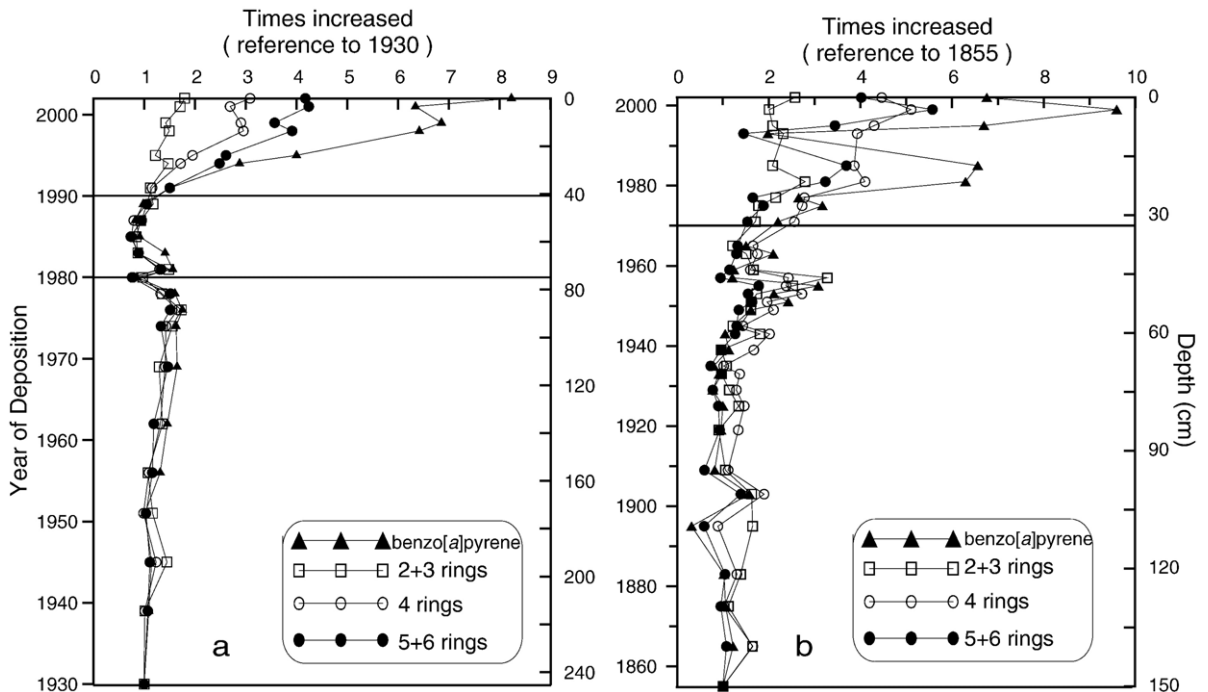

Fig. 6. Annual increased times of fluxes of benzo[a]pyrene and ring groups PAHs in (a) N6 and (b) S5.

High molecular weight (HMW, 5+6 rings) PAHs are products of high temperature combustion involving coal and petroleum such as in power plants and factories, automotive engines and gas-fired cooking utensils (Harrison et al., 1996; Mai et al., 2003). The HMW PAH flux increased faster than the low molecular weight PAHs since the 1990s due to the increase of fossil fuel usage and the transformation from an agriculture economy to an industrial one in China.

The obvious increase in the 16 PAH fluxes in the Yangtze River coastal sea started in the late 1970s in S5 and became more evident after the 1990s in N6 and S5, implying the initiation of nation-wide industrialization. This is in agreement with China's change in energy structure: the increase in coal and oil consumption. This is different from the trends in the United States (Pereira et al., 1999; Lima et al., 2003) and Europe (Fernandez et al., 2000). In the eastern US sediment core, the highest pyrolytic PAH fluxes were in the 1950s with a new peak starting in 1996 (Lima et al., 2003). The decline in pyrogenic PAHs since the 1950s has been attributed to the switch from coal to oil and natural gas as energy source, and the increase since 1996 may be due to the increased usage of diesel fuel by heavy-duty vehicles (Van Metre et al., 2000; Lima et al., 2003). In contrast, the main energy source in China has been, and still is, mainly coal although the usage of petroleum has greatly increased since the 1990s (Guo et al., 2006).

4. Conclusions

The PAHs in the coastal ECS sediment cores have been successfully used to track the economic development stage in that part of China for the past century, even though a strong influence due to the Yangtze River discharge existed at the sampling sites. The variations in PAH concentrations and fluxes were influenced by the floods and dam construction activities of the river. The pronounced increase of 16 PAH fluxes after the 1990s had a close correspondence to the huge economic development in China. The historical variation of PAH flux in the study area is obviously different from the trends in the United States and Europe.

Acknowledgements

References

Bouloubassi I, Fillaux J, Salit A. Hydrocarbons in surface sediments from the Changjiang (Yangtze River) Estuary, East China Sea. Mar Pollut Bull 2001;42:1335–46.

DeMaster DJ, McKee BA, Nittrouer CA, Qian J, Cheng G. Rates of sediment accumulation and particles reworking based on radiochemical measurements from shelf deposits in the East China Sea. Cont Shelf Res 1985;4:143–58.

Fernandez P, Vilanova RM, Martinez C, Appleby P, Grimalt JO. The historical record of atmospheric pyrolytic pollution over Europe registered in the remote mountain lakes. Environ Sci Technol 2000;34:1906–13.

Guo ZG, Lin T, Zhang G, Yang ZS, Fang M. High-resolution depositional record of polycyclic aromatic hydrocarbons in the central continental shelf mud of the East China Sea. Environ Sci Technol 2006;40:5304–11.

Harrison RM, Smith DJT, Luhana L. Source apportionment of atmospheric polycyclic aromatic hydrocarbons collected from an urban location in Birmingham, UK. Environ Sci Technol 1996;30:825–32.

Hu DX, Yang ZS. Key marine flux processes of the East China Sea. Beijing: China Ocean Press; 2001. p. 3–24. (in Chinese).

Huh CA, Su CC. Sedimentation dynamics in the East China Sea elucidated from ^{210}Pb, ^{137}Cs and ^{239,240}Pu. Mar Geol 1999;160:183–96.

Lima AL, Eglinton TI, Reddy CM. High-resolution record of pyrogenic polycyclic aromatic hydrocarbon deposition during the 20th century. Environ Sci Technol 2003;37:53–61.

Lima AL, Farrington JW, Reddy CM. Combustion-derived polycyclic aromatic hydrocarbons in the environment - a review. Environ Forensics 2005;6:109–31.

Liu M, Baugh PJ, Hutchinson SM, Yu L, Xu S. Historical record and sources of polycyclic aromatic hydrocarbons in core sediments from the Yangtze River Estuary, China. Environ Pollut 2000;110:357–65.

Mai BX, Qi SH, Zeng EY, Yang QS, Zhang G, Fu JM, et al. Distribution of polycyclic aromatic hydrocarbons in the coastal region off Macao, China: assessment of input sources and transport pathways using compositional analysis. Environ Sci Technol 2003;37:4855–63.

Oros DR, Ross JRM. Polycyclic aromatic hydrocarbons in San Francisco Estuary sediments. Mar Chem 2004;86:169–84.

Pereira WE, Hostettler FD, Luoma SN, Van Geen A, Fuller CC, Anima RJ. Sedimentary record of anthropogenic and biogenic polycyclic aromatic hydrocarbons in San Francisco Bay, California. Mar Chem 1999;64:99–113.

Van Metre PC, Mahler BJ, Furlong ET. Urban sprawl leaves its PAH signature. Environ Sci Technol 2000;34:4064–70.

Venkatesan MI. Occurrence and possible sources of perylene in marine sediments — a review. Mar Chem 1988;25:1–27.

Wu YH, Wang SM, Hou XH. Chronology of Holocene lastrine sediments in Co Ngoin, central Tibetan Plateau. Sci China 2006;49:991–1001 (D-Earth Sciences).

Xu SS, Liu WX, Tao S. Emissions of polycyclic aromatic hydrocarbons in China. Environ Sci Technol 2006;40:702–8.

Yang Z, Wang H, Saito Y, Milliman JD, Xu K, Qiao S, et al. Dam impacts on the Changjiang (Yangtze) River sediment discharge to the sea: the past 55 years and after the Three Gorges Dam. Water Resour Res 2006;42:W04407.

Yunker MB, Macdonald RW, Vingarzan R, Mitchell RH, Goyette D, Sylvestre S. PAHs in the Fraser River Basin: a critical appraisal of PAH ratios as indicators of PAH source and composition. Org Geochem 2002;32:489–515.

Zhang G, Parker A, House A, Mai BX, Li XD, Kang YH, et al. Sedimentary records of DDT and HCH in the Pearl River Delta, South China. Environ Sci Technol 2002;36:3671–7.